# Hard X-Ray Time Lags from a Seyfert 2

Andrew Lobban

University of Leicester, U.K.

'The X-Ray Universe'

Trinity College, Dublin, Ireland, 17/06/14

In collaboration with:

- William Alston; Institute of Astronomy, Cambridge, U.K.
- Simon Vaughan; University of Leicester, U.K.

# X-Ray Variability

- Many AGN display strong-amplitude X-ray spectral variability
- Both short (~ks) and long (days-weeks-months?) timescales
- Spectrum typically hardens when flux drops

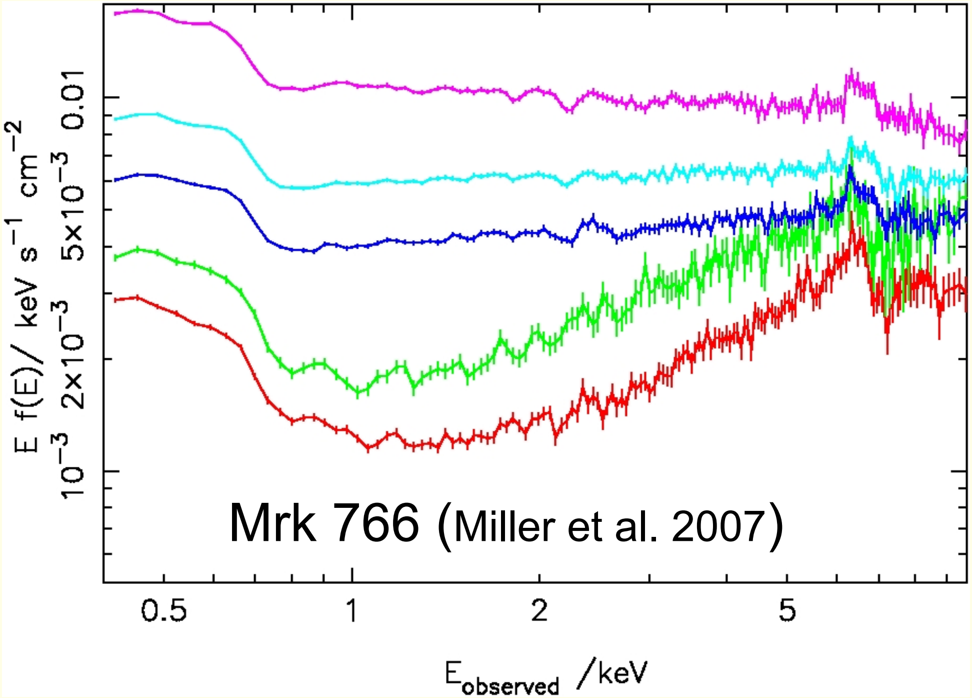


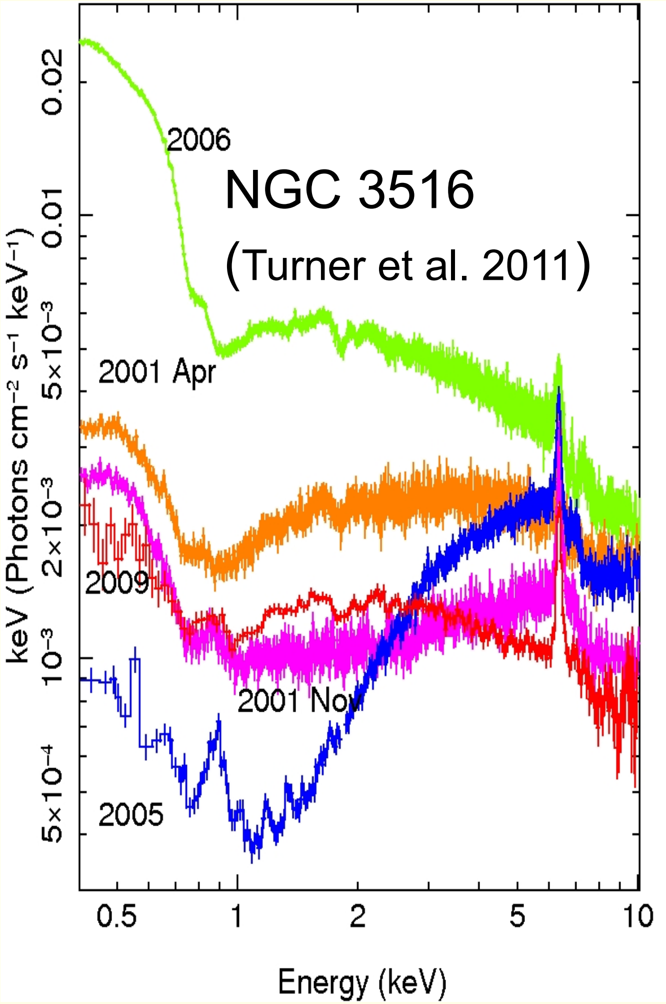

# X-Ray Time Lags

- Computed by comparing cross-spectral products between two energy bands
- Primarily utilising data from XMM-Newton (EPIC-pn) and RXTE
- Hard lags (‘hard’ lagging ‘soft’) as function of Fourier frequency first seen in X-ray binaries – now known to be very common

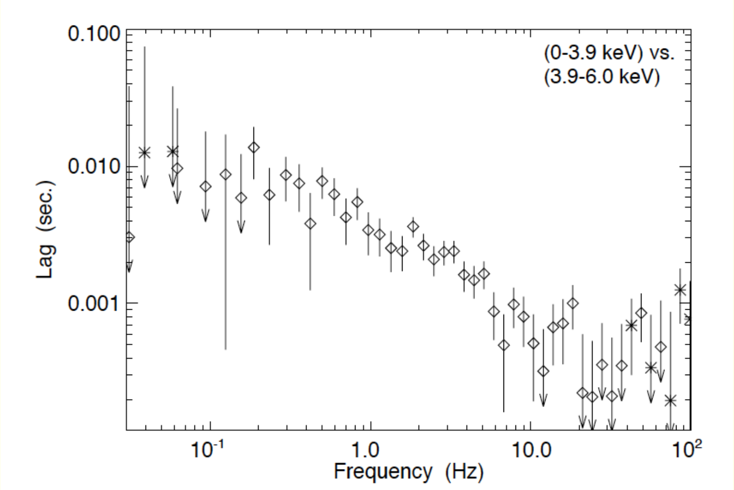


- Cygnus X-1 (Nowak et al. 1999)

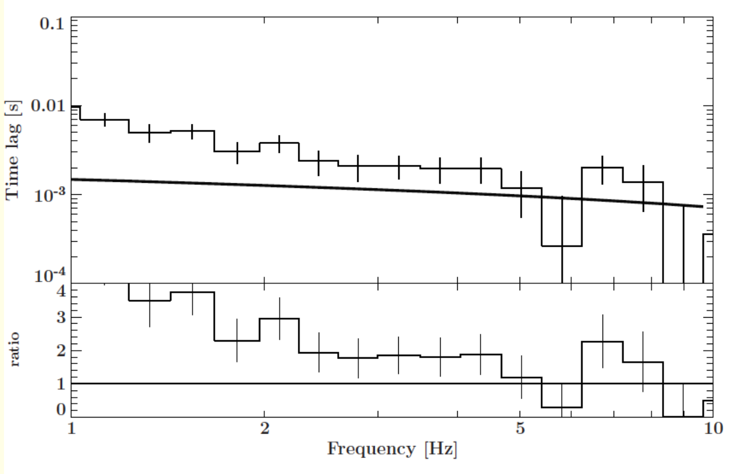


- GX 339-4 (Uttley et al. 2011)

# X-Ray Time Lags

- Discovered in AGN – timescale and magnitude of time delay scaled up due to black hole mass
  - Also, discovery of 'soft' lags at higher frequencies (perhaps associated with reflection / Fe K features)

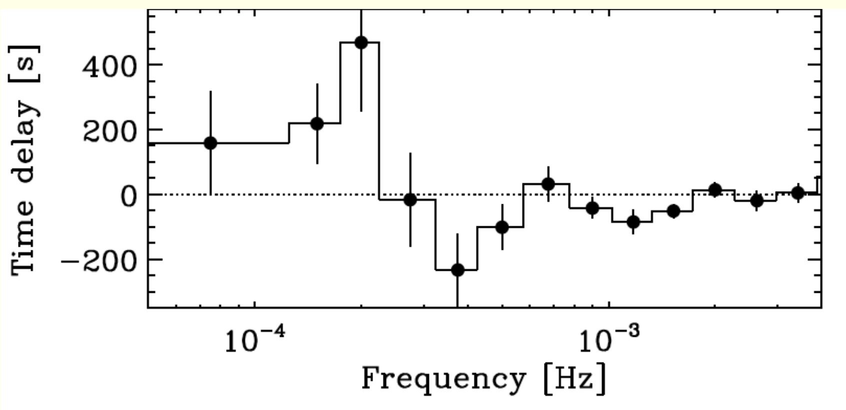


- PG 1244+026 (Alston, Done & Vaughan 2014)
- Ark 564 (Kara et al. 2013)

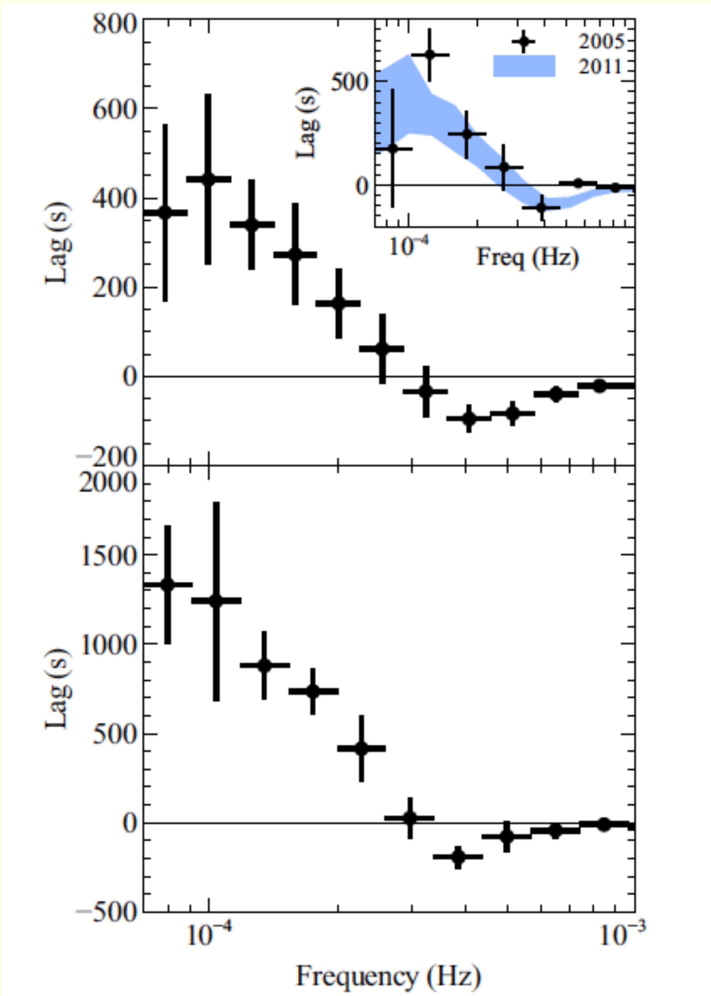

# Variability Mechanisms I: Intrinsic Variability

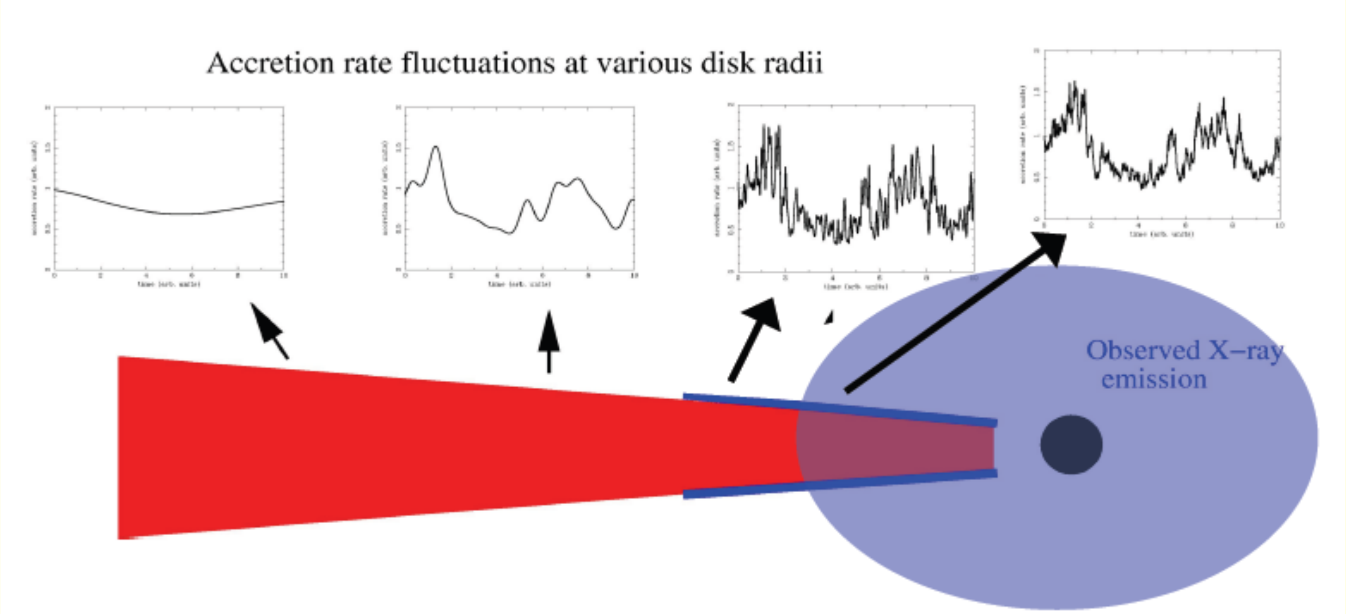


- Leading model: propagating fluctuations in accretion flow (Lyubarskii 1997; Arevalo & Uttley 2006)
- Inward-moving random fluctuations modulate rapid X-ray variations
- Outer corona excited first; fluctuations move inwards exciting harder X-ray-producing region at smaller radii
- Reproduces many observed variability patterns; e.g. time lags / rms-flux

# Variability Mechanisms II: Reprocessing

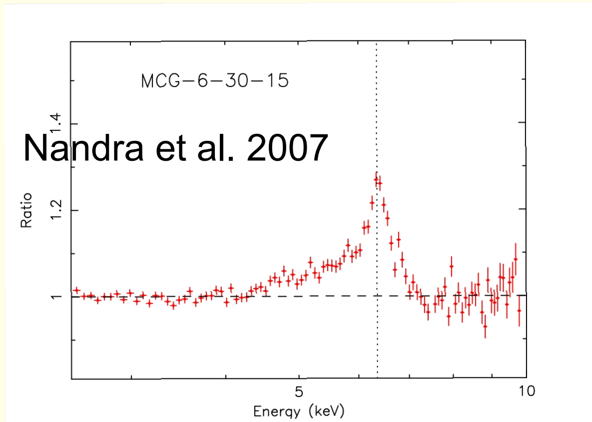


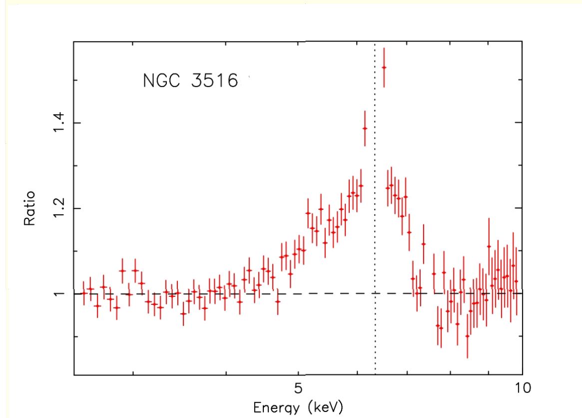


- Motivated by discovery of strong spectral curvature from 2-8 keV
- 'Red wing' not observed to vary in phase with continuum – light-bending (e.g. Miniutti & Fabian 2004)?
- Broad 'red wing' from Fe (gravitational redshift)?

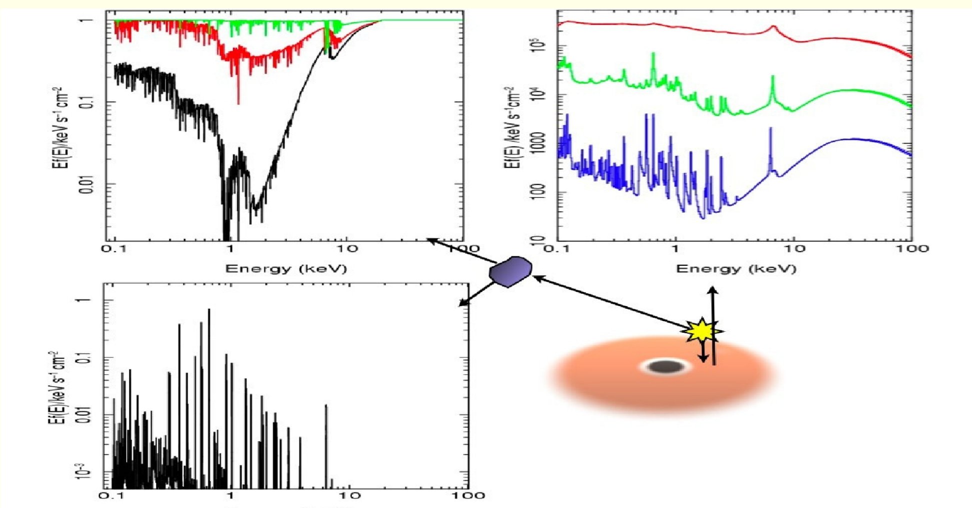


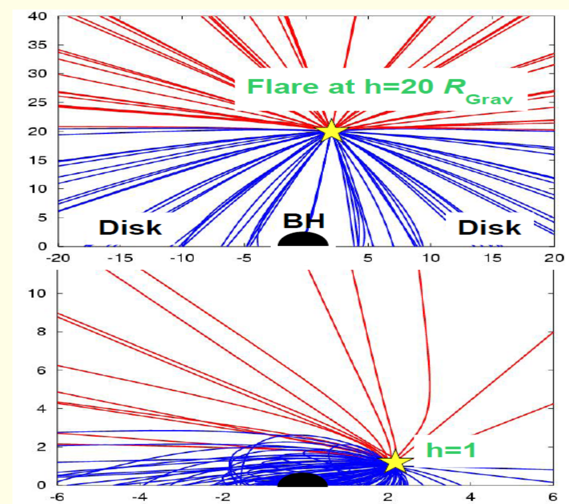


- Transmission / scattering / reflection (Turner & Miller 2009): partial-covering?

# IRAS 18325-5926

- Compton-thin Seyfert 1.9 / Seyfert 2 ($N_H \sim 10^{22}$ cm$^{-2}$)
- Redshift: z=0.01982
- $M_{BH} \sim 10^{6-7} M_{\odot}$
- $L_{2-10} \sim 10^{43}$ erg s$^{-1}$
- Possibly first Seyfert 2 with a claim of a broad Fe line

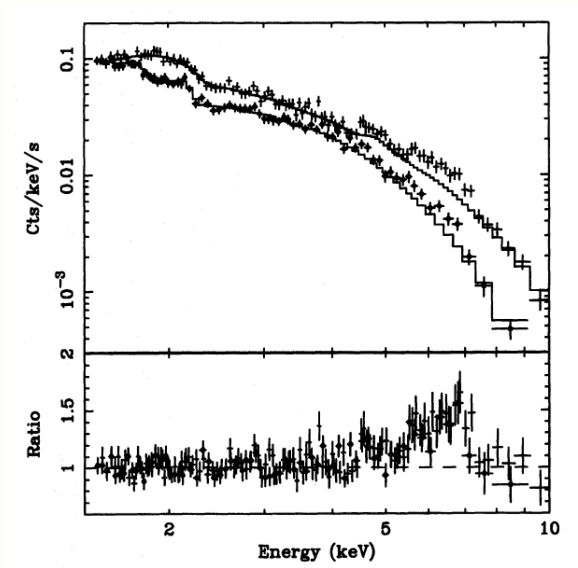


- IRAS 18325-5926 (Iwasawa et al. 1996)

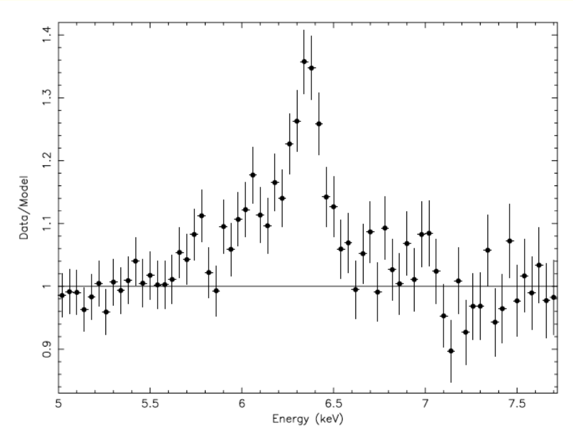


- MCG-5-23-26 (Dewangan et al. 2003)

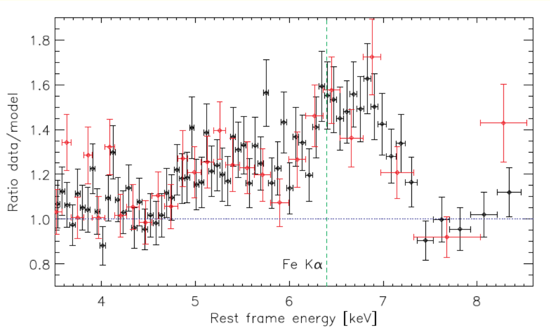


- IRAS 00521-7054 (Ricci et al. in prep.)

# IRAS 18325-5926

- Only stand-alone models for Fe emission fitted to date
- Lobban & Vaughan (2014): Broad-band spectrum from Suzaku (2006) and XMM-Newton (2001)

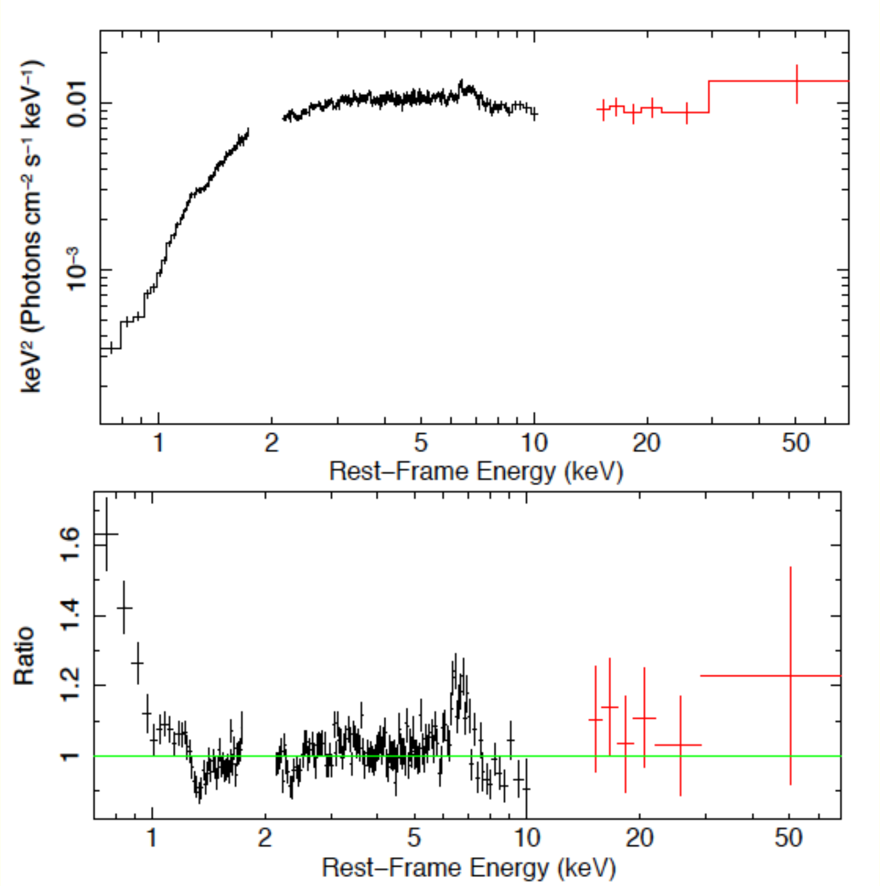


- Power law ($\Gamma \sim 2.2$); neutral absorption ($N_H \sim 10^{22} cm^{-2}$); scattered power law dominating < 0.7 keV

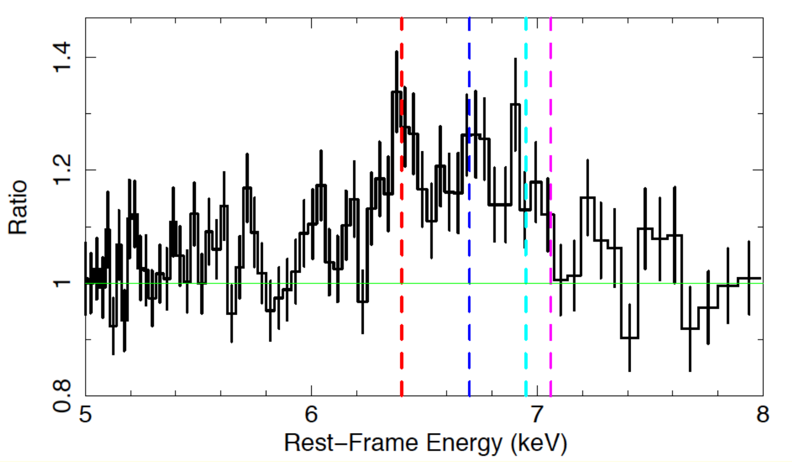


- Fe complex has structure: peaks at ~6.4, ~6.7 & ~6.9 keV -> a blend of narrow lines?

# IRAS 18325-5926

- Can fit with blurred, relativistic reflection down to 6$r_g$ -> emission peaks at ~6.7 keV and suggests origin in ionised accretion disc
- Narrow, photoionised emission lines (Xstar) give statistically comparable fit (5.5-7.5 keV) to blurred relativistic ionised reflection -> highly ionised (log$\xi$ ~ 3.5): dominated by H-like and He-like Fe; high column: > 3 x $10^{23}$ cm$^{-2}$
- He-like Fe EW ~30 eV -> consistent with predictions for photoionised gas from Bianchi & Matt (2002)

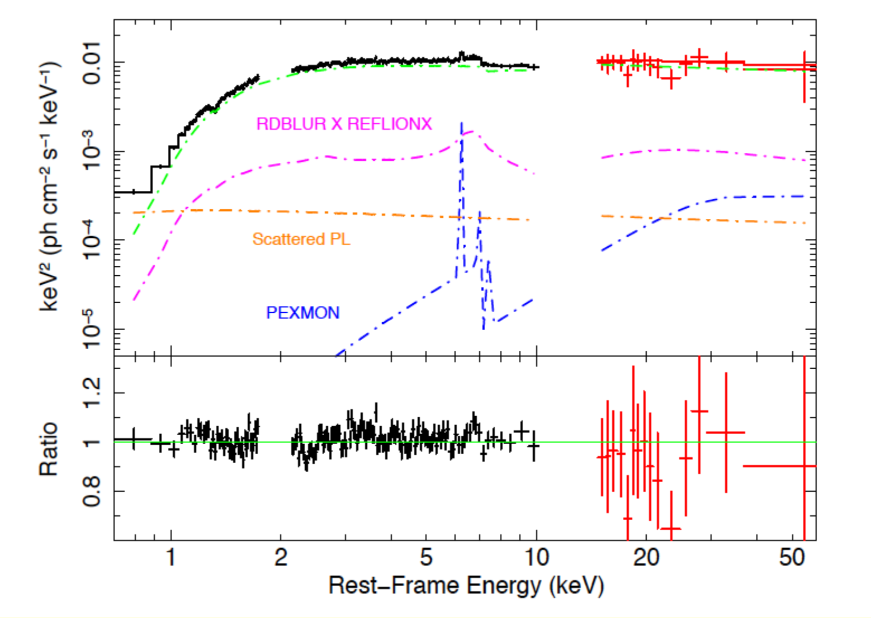


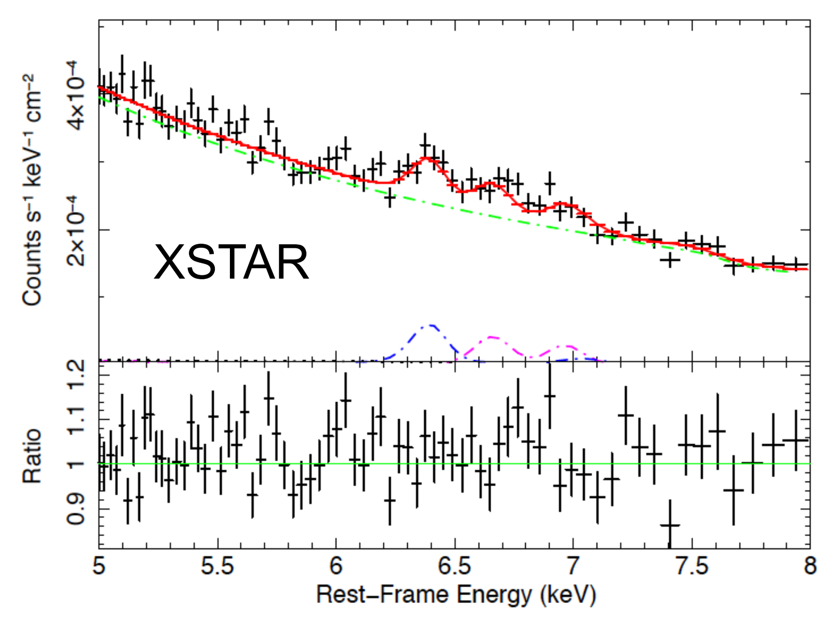

# 200ks New XMM-Newton Data

- Two orbits: 100ks each

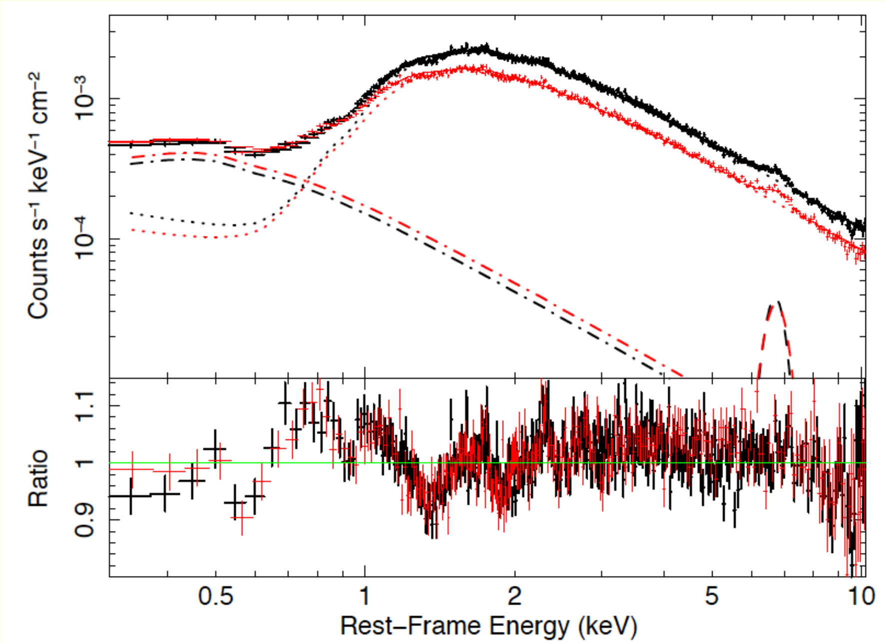


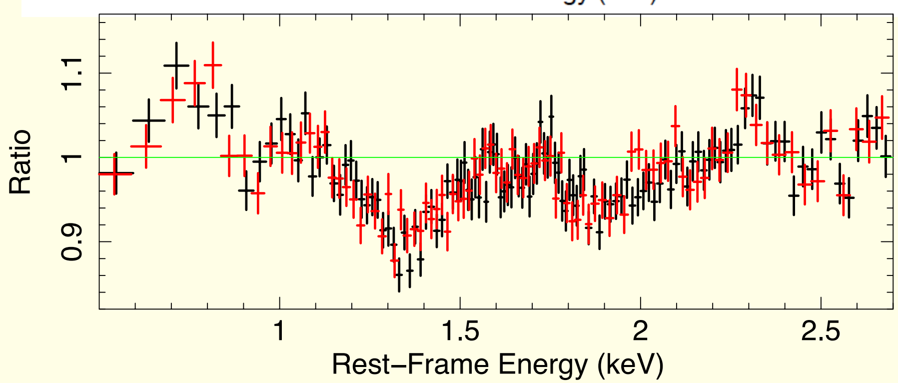


- Intrinsic power law modified by neutral absorption + scattered power law + Fe emission
- Spectral properties similar to Suzaku data
- Long-term spectral changes dominated by power-law normalisation
- No strong soft excess
- ‘Absorption’ feature at ~1.3 keV: consistent with Mg XI but broad (FWHM ~30000 km/s) – absorption grids massively overpredict other features
- Instead, fit with broken power law: weak soft excess may be hidden in spectrum

# Significant Short-Term Variability

- 0.2-10 keV lightcurve: varies by a factor of ~3 on tens of ks
- Averaged rms spectrum: 29 energy bands extracted over four 50ks segments with 1ks time resolution
- Computed fractional excess variance, averaged over segments
- Computed fractional rms by taking square root of excess variance
- Very little variability <0.7 keV (dominated by distant scattered component) -> exclude data <0.7 keV in subsequent analysis

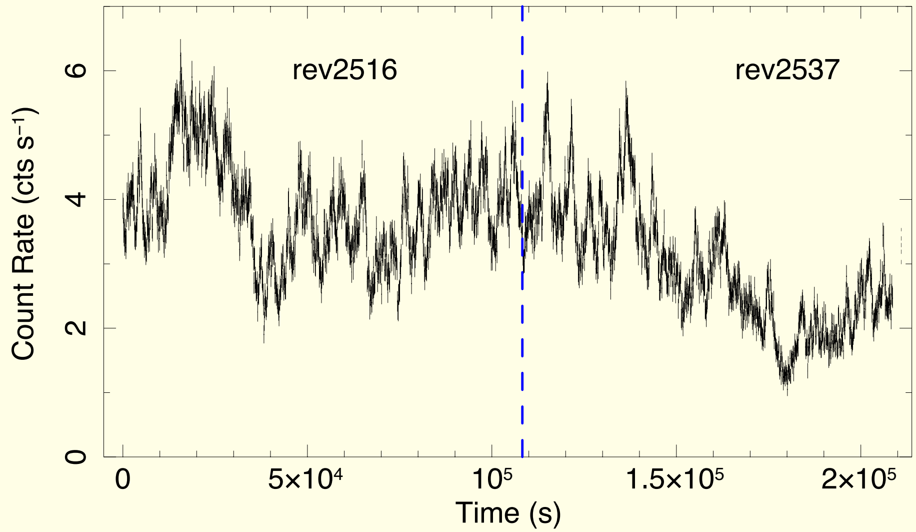


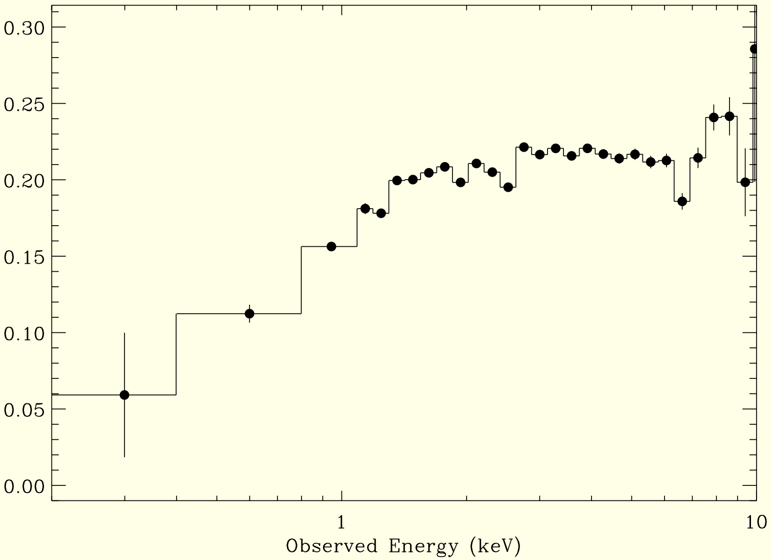

# Frequency-Dependent Time Lags

- Combined EPIC MOS + pn data
- 0.7-1.5 keV vs 2.5-10 keV
- 4 50ks segments -> compute discrete Fourier transforms and combine to form cross-periodograms -> average over 4 segments
- Methods described in Vaughan & Nowak (1997), Nowak et al. (1999), Vaughan et al. (2003), Uttley et al. (2011)
- Hard lag increasing in magnitude at lower frequencies
- High coherence up to $10^{-3}$ Hz (coherence of 1 means variability in one band can be perfectly predicted in another)
- Flux-dependence: lag increases with source flux

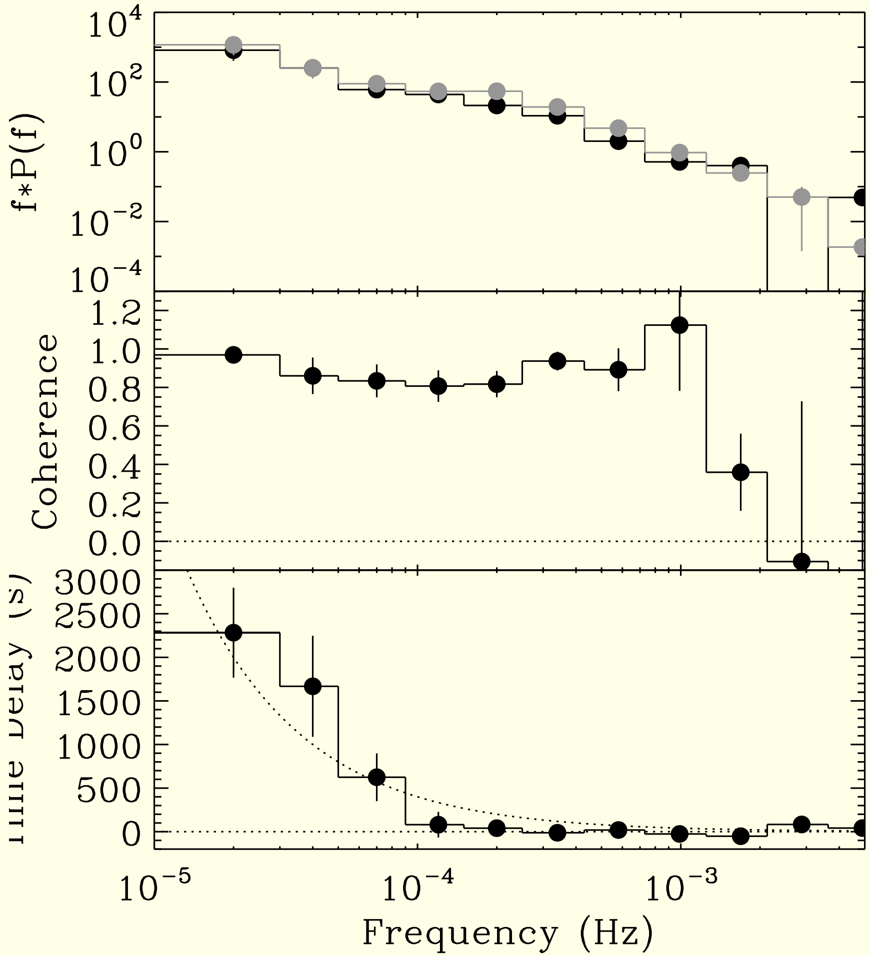

# Low-Frequency Lag-Energy Spectra

- Energy-dependence of lags
- Calculated over a given frequency range for a series of consecutive energy bands against broad reference band (e.g. 0.7-1.5 keV)
- At lowest frequencies, lag scales approximately linearly with separation of energy band -> similar to Cygnus X-1 and GX 339-4
- One of the first lag-energy spectra from Seyfert 2 (also see MCG-5-23-16 and NGC 7314; Zoghbi et al. 2013, 2014)

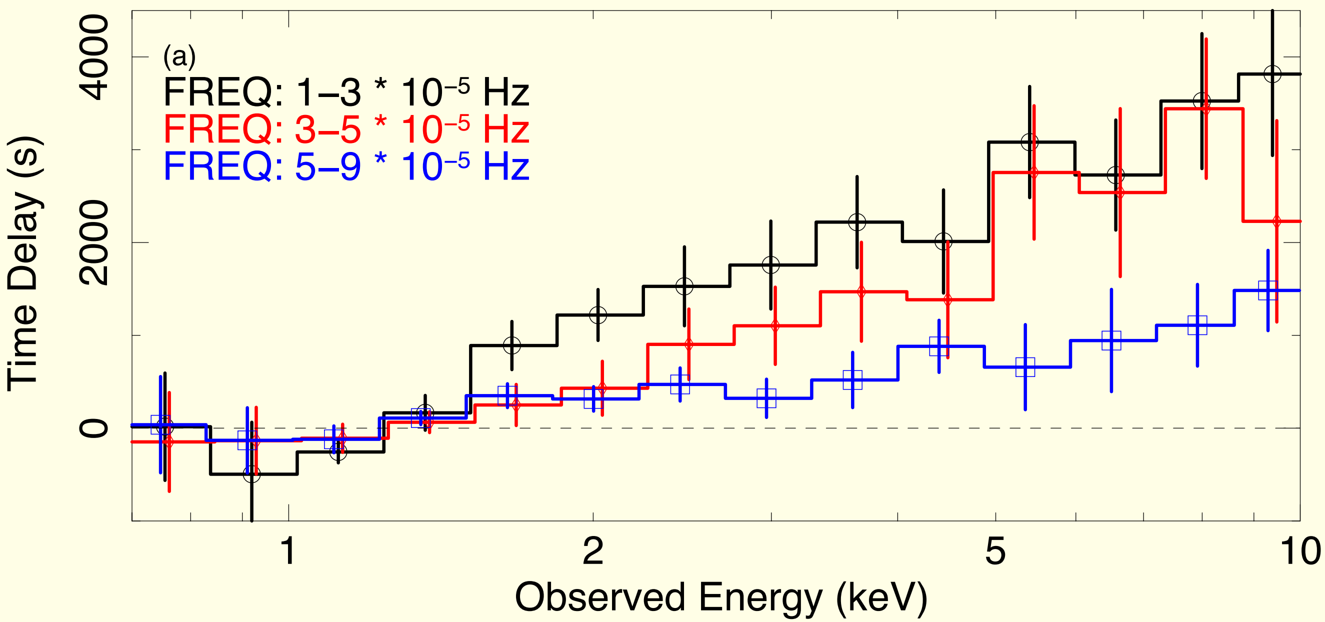

# Fitting the Lag-Energy Spectra

- Fitting reprocessing models:
- Assume primary, p(E), and reprocessed (delayed), r(E), spectra
- Assume top-hat function as simple time-shifted response
- Essentially normalise shape of TH impulse response according to shape of delayed spectrum relative to primary spectrum
- Phase lag (see Uttley et al. 2014):

$$\phi(\omega) = \arctan\left(\frac{R\sin(\omega\tau_0)\mathrm{sinc}(\omega\Delta\tau/2)}{1 + R\cos(\omega\tau_0)\mathrm{sinc}(\omega\Delta\tau/2)}\right)$$

- Here, R is the ratio of reprocessed / primary emission (α)
- Time delay between bands:

$$\tau(f, E_j, E_i) = \frac{1}{2\pi f}(\phi_j(f) - \phi_i(f))$$

- Can fit using two free parameters: central delay, $\tau_0$ and α
- Assume $\Delta\tau = 2\tau_0$ (i.e. a spherical shell type of reprocessor)
- Compute spectral ratio, r(E)/p(E) and optimise free parameters, $\tau_0$ and α, to give best fit
- Each fit performed by integrating over each energy bin with same binning as lag-energy spectra (high-resolution forms shown in plots)

# Fitting the Lag-Energy Spectra

- Neutral reflection: p(E) = power law; r(E) = PEXMON (R = 1)
- Best-fitting values from spectral fits
- $X^2$ / d.o.f. = 96.5 / 40 ($p = 1.4 \times 10^{-6}$)
- $\tau_0$ = 2.2 ks; α = 35.7 (inconsistent with time-averaged spectrum)
- Harder bands are reflection dominated (at high α, $\tau \sim \tau_0$ – lag saturates > 5 keV -> diluted Fe emission line)

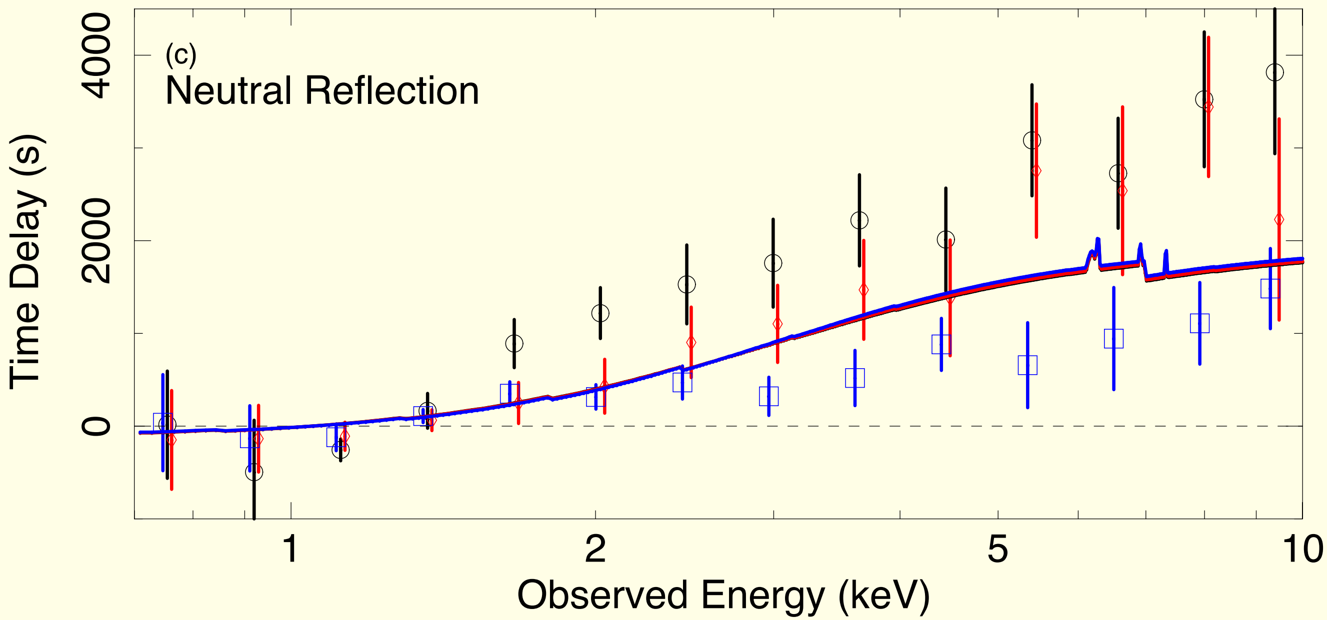

# Fitting the Lag-Energy Spectra

- Ionised reflection: p(E) = power law; r(E) = RDBLUR x REFLIONX (R ~ 1)
- Best-fitting values from spectral fits (log $\xi \sim 10^3$)
- $X^2$ / d.o.f. = 327 / 40 (no better than a constant)
- If $\tau_0$ roams freely, $X^2$ / d.o.f. = 114.5 / 40; $\tau_0$ = 39 ks; $\alpha$ = 5.4
- At frequencies > $2/\tau_0$, lag sign in cross-spectrum 'flips' (at a given Fourier frequency, phase difference is constrained within [$-\pi$,$+\pi$]; a shift of +3/4 wavelengths indistinguishable from -1/4 (see Miller et al. 2010 / Zoghbi et al. 2011)

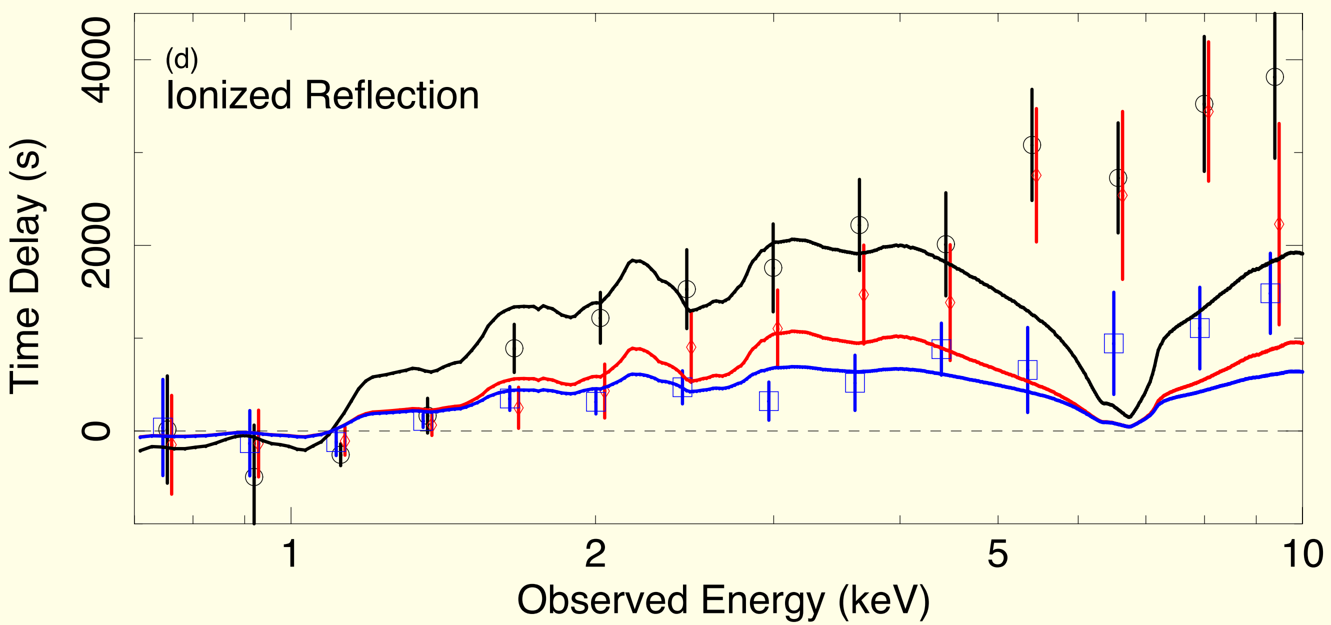

# Fitting the Lag-Energy Spectra

- Neutral absorption: p(E) = power law; r(E) = TBABS*power-law
- A range of column densities from $10^{21\text{-}24}$ $cm^{-2}$
- Best fit: $3 \times 10^{22}$ $cm^{-2}$; $X^2$ / d.o.f. = 38.1 / 40 (p = 0.56)
- $\tau_0$ = 6.4 ks; $\alpha$ = 0.67
- Adding this absorber to spectral model improves fit by $\Delta X^2 \sim 400$ and is ~50 per cent weaker (compare with $\alpha$)

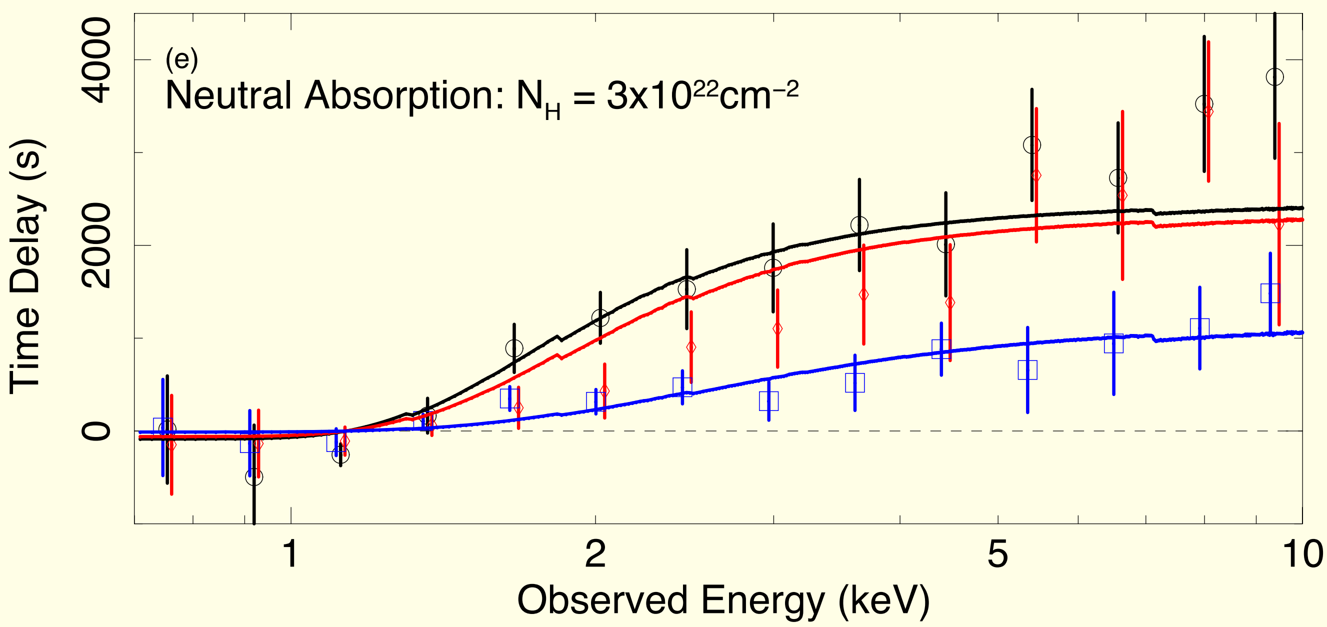

# Fitting the Lag-Energy Spectra

- Simple log-linear model including $f^{-1}$ dependence on frequency:
- $\tau(E,f) = A(f/f_0)^{-1} \log(E) + B$
- Fixed $f_0$ at $2 \times 10^{-5}$ Hz (central frequency of lowest bin)
- $X^2$ / d.o.f. = 33.8 / 40
- Log-linear lag-energy shape may be expected from propagating fluctuations model (Kotov et al. 2001; Arevalo & Uttley 2006)

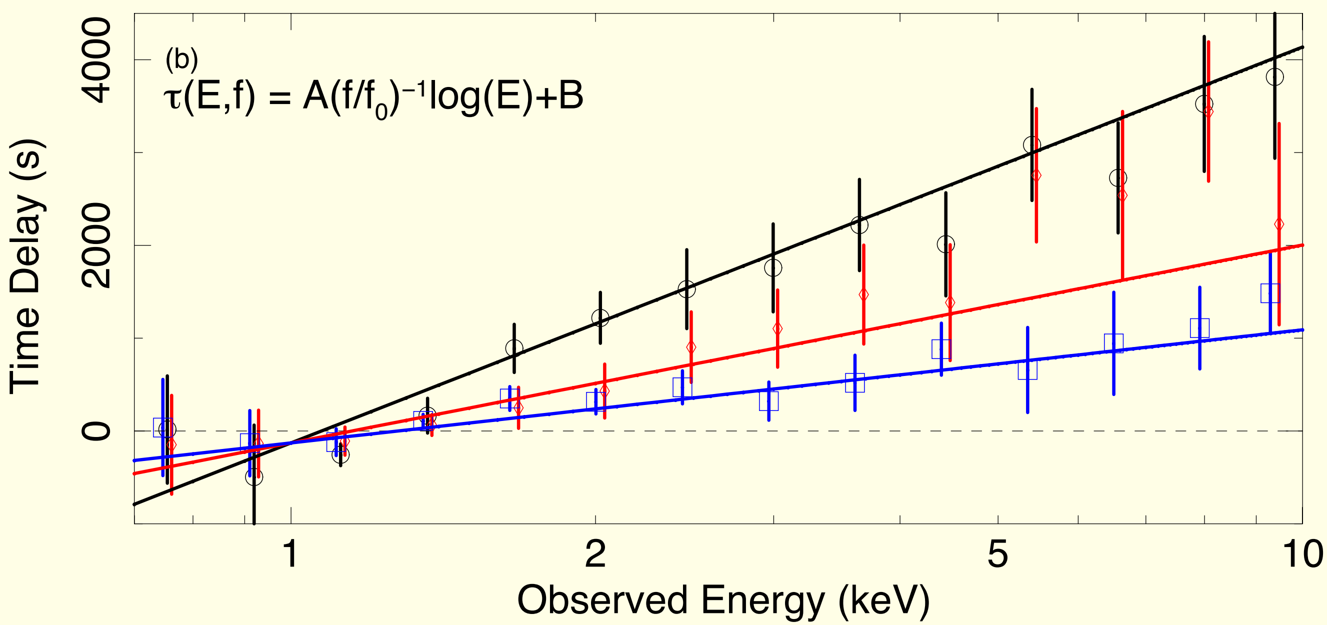

# Summary

- Hard lag: hard band lagging soft band by up to ~3ks
- Clear energy-dependence of the lag, increasing approx. linearly with the log of the separation of the energy bands
- Log-linear model and neutral absorption give good fits
- Energy-dependence of the PSD is a challenge for the reprocessing models: if hard spectrum with long delay produce hard lags, variations in reprocessed light should be delayed and smoothed -> smoothing should steepen PSD at high frequencies (timescales < $\tau_0$)
- Findings similar to Cygnus X-1 (Kotov et al. 2001) and other AGN (McHardy et al. 2004)– similarity suggests similar mechanism at work between AGN and XRBs: most likely due to propagating fluctuations within accretion flow
- Low-frequency hard lags may be ubiquitous – hotly debated soft lags may not be -> it Is crucial to understand hard lags if we are to disentangle them from intriguing soft lags
- Lag-energy models will look different if frequency-/energy-range extended; e.g. absorber should show constant lag-energy spectrum at higher energies while prop. fluc. model may increase further -> setting the scene for more future observations with NuStar